Book Chapter

Electrodeposition of high entropy alloy coating: A brief of the deposition parameters

Ashwin Shah*, Banti Chauhan*, Rajesh Kumar Rai*, Brij Mohan Mundotiya*

*Department of Metallurgical and Material Engineering MNIT Jaipur, Rajasthan, India

Abstract

The electrodeposition of high entropy alloys (HEAs) is a promising avenue of research for multicomponent alloy coatings. It offers simplicity, uses readily available materials, and operates at ambient temperatures. The process allows controlled microstructure and composition through parameter modulation. Electrodeposition provides versatility, cost-effectiveness, and environmental sustainability compared to conventional methods. It presents a transformative approach to fabricating HEA coatings for various applications, offering tailored compositions and improved properties.

1. Introduction

High entropy alloys (HEA) comprise at least five elements, often in equal atomic ratios or ranging from 5 to 35 at.% of the principle elements [1, 2]. Despite expecting complex or intermetallic structure, these alloys exhibit high mixing entropy, resulting in a lower free energy state and simple cubic crystal structures leading to exceptional mechanical, corrosion, thermal, tribological, damping, irradiation, and magnetic properties surpassing those of conventional alloys [3, 4]. The unique attributes of high entropy alloys have garnered interest across various industries, such as nuclear, chemical plants, marine, aerospace, and gas turbine applications [5, 6].

Various methods have been employed to produce high entropy alloys, each offering unique advantages [8]. Liquid-phase routes include techniques like arc and induction melting, laser melting, electric resistance melting, thermal spray, and laser cladding. At the same time, gas-phase methods encompass molecular-beam epitaxy, vapor deposition, magnetron sputtering, pulsed laser deposition, and atomic layer deposition. Solid-phase techniques, such as mechanical alloying and chemical processes like Sol-Gel, have also been employed for HEA synthesis [4].

Among these techniques, electrodeposition has emerged as an attractive and promising method for high entropy alloy synthesis[7, 8]. This technique has garnered considerable attention due to its cost-effectiveness, availability of raw materials, and relative simplicity compared to other methods. Moreover, electrodeposition allows for the easy tuning of various properties of coatings by manipulating current density, applied potential, and bath conditions [9]. Electrodeposition's versatility and ability to produce tailored coatings with enhanced properties hold great potential for high entropy alloy synthesis and applications [10].

Despite the promising results, the electrodeposition of high entropy alloys presents several challenges. Precise control of multiple metallic precursors with differing reduction potentials is essential to achieve the desired alloy composition. Additionally, unwanted secondary phases and compositional inhomogeneity formation require careful attention. This section addresses these challenges and discusses potential strategies to overcome them, such as pulse electrodeposition, alternative electrolytes, and advanced modeling techniques. The chapter concludes with an outlook on future research directions and the potential of electrodeposited high entropy alloy coatings in advancing materials science and engineering.

2. Electrodeposition of High Entropy alloy

2.1 Electrodeposition Process

The electrodeposition process involves immersing the substrate (cathode) and the counter electrode (anode) into the prepared electrolyte bath. The substrate is the receiving surface for the high entropy alloy coating deposition. The counter electrode, typically made of a material that does not participate in the deposit generally (platinum and graphite electrode), completes the electrochemical circuit. Redox (oxidation-reduction) processes are the fundamental building blocks of this technique. This technique uses four main components of an electrolytic cell: an anode, a cathode, an electrolyte, and a power supply. Oxidation reactions occur at the anode, whereas reduction reactions occur at the cathode [11]. The coating medium is an electrolyte consisting of an electrochemical solution of metal salts. When an external current from a power source is applied to the electrodes, reactions (1) and (2) take place simultaneously,

$$M^{n+} + ne^- \rightarrow M\ (at\ cathode) \qquad (1)$$

$$M \rightarrow M^{n+} + ne^-\ (at\ anode) \qquad (2)$$

The reduction reaction of metal ions was thought to proceed in two steps as follows:

$$M(II) + e^- \rightarrow M(I)_{adsorbed}$$

$$M(I)_{adsorbed} + e^- \rightarrow M_{atom}$$

Where M stands for the preferred metals, this section delves into the fundamental principles of electrodeposition, nucleation and growth mechanism, and electrolyte preparation and discusses the influence of deposition parameters.

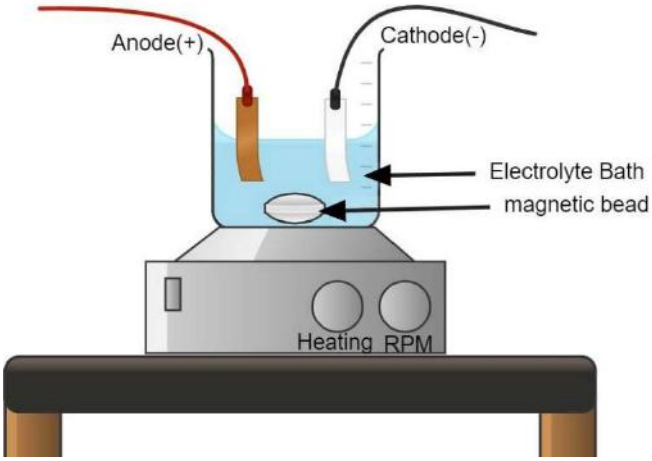

Figure 1. Schematic of electrodeposition setup

2.2 Growth and nucleation mechanisms

Nucleation and growth mechanisms are paramount in the electrodeposition process of alloy films on a conductive substrate. Nucleation, in particular, plays a critical role as it governs the subsequent evolution of the microstructure and crystallinity in the deposited alloy film [12]. During electrodeposition, the formation of the alloy film on the conductive substrate occurs through a heterogeneous process. The interface between the electrolyte solution and the substrate surface serves as the primary region for nucleation, providing preferential sites for the nucleation of metal ions. The metal ions in the electrolyte are drawn to the charged substrate (cathode), where they gain electrons and undergo reduction, resulting in nuclei composed of metal atoms. The nucleation process has a considerable impact on the overall structure and properties of the deposited alloy film. As the nucleated nuclei continue to grow, they act as sites for the additional deposition of metal atoms, contributing to the growth of the film [13]. The alloy film gradually

thickens due to the electrodeposition process, and the nucleation and growth mechanisms determine the final microstructure and crystallinity. The growth mechanism in electrodeposition can occur in different modes: (a) layer-by-layer growth, (b) island growth, and (c) island-layer growth. Layer-by-layer growth involves the sequential deposition of metal atoms, forming well-defined and smooth film layers.

In contrast, island growth occurs when metal atoms form separate islands on the substrate surface, which coalesce to create a continuous film [14]. The island growth results when the cohesion between the atoms of the deposited material is higher than the adhesion between deposited atoms and substrate; hence, a cluster is formed. In the island-layer growth mode, one or two monolayers initially form before starting the island's growth on the substrate surface.

2.3 Electrolyte Preparation

The successful electrodeposition of high entropy alloys hinges on preparing a well-tailored electrolyte. The first step in this process is to select the appropriate metal precursors and other compatible additives to form the desired alloy composition. These components are then dissolved in an aqueous medium, considering their solubility and stability in the electrolyte solution. Achieving the "right proportion" of elements is critical because it ensures consistent coverage of each element in the deposited coating, resulting in a balanced equiatomic composition. This section explores various methods of electrolyte preparation, including the dissolution of salts, complexing agents, and pH adjustment, focusing on optimizing the deposition process. The metallic salts are generally composed of chloride-based, sulfate and phosphate-based.

2.4 Additives

In the context of a HEA film, the significant differences in reduction potentials among its constituent elements can lead to morphological instabilities and compositional challenges during the electrodeposition process. The complex interaction of reduction potentials among the alloy's numerous elements might result in the preferential deposition of some elements over others. This may cause the elements to be distributed unevenly in the deposited film, departing from the HEA's intended composition. Consequently, achieving both morphological stability and the desired compositional uniformity in the HEA film through the co-deposition of all constituents becomes a

complex task under these conditions. The standard reduction potential of the elements is represented in Fig 2 and given in Table 1.

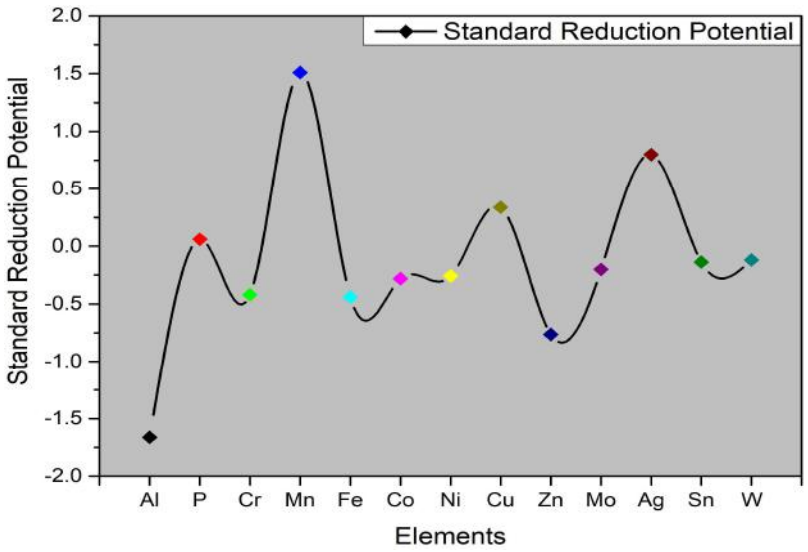

Figure 2. Standard reduction potential

Table 1. The standard reduction potential of elements

Elements	Al	P	Cr	Mn	Fe	Co	Ni	Cu	Zn	Mo	Sn	W
Standard reduction potential	-1.662	0.06	-0.42	1.510	-0.440	-0.280	-0.257	0.337	-0.763	-0.2	-0.136	-0.119

The successful electrodeposition of HEAs demands the inclusion of several additives in the electrolyte, each serving specific functions to ensure optimal deposition outcomes. These additives significantly impact the overall electrodeposition process by controlling reduction potentials. In the context of HEAs, a range of additives are employed to address various electrochemical and deposition challenges. One such common additive is boric acid, which acts as a buffer agent, helping to stabilize the pH of the electrolyte solution. Gelatine is a bonding agent, promoting adhesion between the substrate and the deposited alloy. Sulfanilic acid is introduced to dissolve the gelatine, enabling its effective utilization.

Additionally, formic acid finds utility in enhancing the surface morphology of the deposited film. Its presence contributes to achieving a smoother, more uniform surface, impacting the film's properties and performance. Sodium dodecyl sulfate is often incorporated to reduce the surface tension on the cathode surface, facilitating a controlled deposition process. Potassium chloride and

ammonium chloride are introduced to enhance solution conductivity, thus ensuring efficient charge transfer during electrodeposition. Moreover, L-ascorbic acid serves a critical role in hindering the formation of hydroxides, which could otherwise adversely affect the quality of the deposited HEA film. These additives highlight the complex interaction of electrochemical kinetics and their profound impact on deposition processes. The careful selection and manipulation of these additives enable researchers to tailor the electrodeposition process. HEA films with the desired properties and consistent compositional homogeneity are therefore produced. As the field of HEA research evolves, the continued exploration and refinement of such additive strategies promise to unlock new avenues for advancing the capabilities and applications of these remarkable materials.

3. Electrolyte bath

Different types of baths are used, such as organic baths, ionic baths, cyanide-based baths, and aqueous baths; all have their merits and demerits of use. The electrodeposition of high entropy alloy (HEA) coatings has witnessed extensive usage of both aqueous electrolyte baths [15] and organic electrolyte baths, incorporating organic solvents like DMF (Dimethylformamide) and CH_3CN (Acetonitrile) [16], each providing distinct advantages for specific applications.

Aqueous baths utilize deionized water as the solvent, rendering them cost-effective, environmentally friendly, and readily available. The aqueous nature ensures thermal stability and safe handling, reducing concerns related to flammable or toxic solvents. Researchers have demonstrated the flexibility of aqueous baths by adjusting the concentration of metal salts or incorporating specific additives to customize the properties of the deposited coatings [17-20].

In contrast, using DMF and CH_3CN as solvents, organic electrolyte baths offer specific advantages during electrodeposition. These baths exhibit excellent solvating power, facilitating the efficient dissolution of metal salts and precursor compounds. The enhanced mass transfer of metal ions in organic baths contributes to improved adhesion and mechanical properties of HEA coatings. Additionally, the broader electrochemical window of organic baths allows a wider range of applied voltages without significant decomposition [21]. For instance, Aliyu et al. [22] researched electroplating Cu-Fe-Ni-Co-Cr HEA coatings with graphene oxide (GO) addition in an aqueous bath, resulting in distinct phases and enhanced corrosion resistance. Similarly, Aliyu and Srivastava [15] investigated Mn-Cr-Fe-Co-Ni HEA coatings with GO addition, revealing improved corrosion resistance and microstructure homogeneity. In aqueous baths, Aliyu et al. [23]

explored Al-Cr-Fe-Co-Ni-Cu HEA coatings with varying GO percentages, aiming to enhance corrosion resistance through uniform Al distribution.

In conclusion, selecting an electrolyte solution for the electrodeposition of HEA coatings, whether aqueous or organic, depends on various factors, such as cost, environmental considerations, and desired qualities. Researchers are optimizing bath parameters in both types to produce well-controlled, homogeneous, and high-performance HEA coatings for diverse industrial applications.

4. Direct current Aqueous bath Electrodeposition

Table 2: Various HEA systems developed by electrodeposition technique.

Alloy	Type of deposition	Electrolyte bath	Crystal structure	Concentration	Ref.
FeCoNiCuZn	DC	Aqueous	FCC	Sulfate based Salts of elements	[20]
AlFeCoNiCu	DC	Aqueous	FCC + BCC	$CoCl_2 \cdot 6H_2O$	[24]
				$AlCl_3 \cdot 6H_2O$	
				$NiCl_2 \cdot 6H_2O$, $FeCl_2 \cdot 4H_2O$,	
				$CuCl_2 \cdot 2H_2O$	
MnCrFeCoNi	DC	Aqueous	BCC	MnCl2·4H2O (29.69 gL–1)	[15]
				FeCl2·4H2O (7.95 gL–1)	
				CrCl3·4H2O (33.30 gL–1)	
				NiCl2·6H2O (19.02 gL–1)	
				CoCl2·6H2O (9.517 gL–1)	
CuFeNiCoCr	DC	Aqueous	BCC + FCC	$CoCl_2 \cdot 6H_2O$ (9.52 gL^{-1})	[22]
				$CuCl_2 \cdot 2H_2O$ (6.82 gL^{-1})	
				$FeCl_2 \cdot 4H_2O$ (7.95 gL^{-1})	
				$NiCl_2 \cdot 6H_2O$ (16.64 gL^{-1})	
				$CrCl_3 \cdot 4H_2O$ (37.30 gL^{-1})	

				Added graphene oxide (GO)	
AlCrFeCoNiCu	DC	Aqueous	BCC + FCC	$CoCl_2 \cdot 6H_2O$ (9.52 gL^{-1})	[25]
				$NiCl_2 \cdot 6H_2O$ (16.64 gL^{-1}) $CuCl_2 \cdot 2H_2O$ (6.82 gL^{-1})	
				$FeCl_2 \cdot 4H_2O$ (7.95 gL^{-1})	
				$CrCl_3 \cdot 4H_2O$ (37.30 gL^{-1})	
				$AlCl_3 \cdot 6H_2O$ (24.14 gL^{-1})	
				Added graphene oxide (GO)	
AlCrFeMnNi & AlCrCuFeMn	DC	(DMSO-$(CH_3)2SO$) - acetonitrile (AN-CH_3CN)	Amorphous (as deposited) BCC (After annealing at 873K for 2h)	$AlCl_3$ (0.016 mol/L)	[26]
				$CrCl_3$ (0.016mol/L)	
				$CuCl_2$ (0.012mol/L)	
				$FeCl_2$ (0.012mol/L)	
				$MnCl_2$ (0.012mol/L)	
				$NiCl_2$ (0.012mol/L)	
FeCoNiCrX (X =Mn, Al)	DC	Aqueous	FCC	$FeSO_4 \cdot 7H_2O$	[7]
				$CoSO_4 \cdot 7H_2O$	
				$NiSO_4 \cdot 7H_2O$	
				$Cr2(SO_4)_3 \cdot 6H_2O$	
				$MnSO_4 \cdot H_2O$	
				$Al2(SO_4)_3 \cdot 18H_2O$	
CoNiWReP	DC and PC	Aqueous	Amorphous	$NiSO_4.6H_2O$ 4 g/L	[27]
				$CoSO_4.7\ H_2O$ 1 g/L	
				$Na_2WO_4.2$ H2O 50 g/L	
				NH_4ReO4 3 g/L as Re	
				$NaH_2PO_2.1$ H2O Varied	
CoCrFeMnNi		(DMSO-$(CH_3)2SO$) acetonitrile (AN-CH_3CN)	Amorphous (as deposited) FCC after heat treatment	$CoCl_2$, $CrCl_3.6H_2O$, $FeCl_2.$ $4H_2O$, $MnCl_2.4H_2O$ and $NiCl_2.6H_2O$	[28]

Table 2 thoroughly reviews various significant research projects concentrating on the electrodeposition of HEAs through aqueous solutions utilizing a direct current (DC). Aliyu et al. have contributed significantly to advancing electrodeposition techniques for High Entropy Alloys (HEAs). Their focus primarily lies in the electrodeposition of HEAs using an aqueous medium and a DC power source. Notably, they have investigated various HEA compositions, including AlFeCoNiCu[24], AlCoCrCuFeNi[23], MnCrFeCoNi[15], CoCrCuFeNi [22], and. Moreover, their research expanded to incorporate graphene oxide (GO) as an additive to these alloys. Through their studies, Aliyu et al. explored the corrosion behavior of HEA-GO composite coatings, observing significant improvements in corrosion resistance. Their work further delved into microstructural alterations within the coating morphology, substantiating the efficacy of graphene oxide in enhancing the overall properties of these HEA coatings. The crystal structure formed in the electrodeposited alloy is FCC, FCC+BCC, and some coatings showed amorphous structure. Also, some researchers have done annealing after they showed crystal structure. Along with Aliyu et al.'s contributions, the table highlights the incredible research projects, each offering a distinct perspective on understanding electrodeposition procedures for HEAs. Along with aliyu et al.'s contributions, the table highlights the incredible range of studies, each offering a distinct perspective on how electrodeposition procedures for HEAs are understood.

5. Deposition Parameters

Precise control of deposition parameters is essential to achieve specific microstructural and compositional features in the electrodeposited high entropy alloy coatings. The deposition current density, bath temperature, pH level, and agitation are critical factors that affect the growth kinetics, crystallographic orientation, and grain size of the coatings. This section examines the influence of each parameter on the properties of the deposited coatings, offering insights into the optimization of the electrodeposition process. The following are some of the main results of different processing parameters:

5.1 Deposition Current Density

Current density is the critical parameter in the electrodeposition, significantly impacting the composition, morphology, and mechanical properties of the electrodeposited coating. Ghaferi et al. [29] conducted a comprehensive investigation on the effects of various current densities (10, 20, 35, and 50 mA/cm^2) in the electrodeposition of FeCoW coating. Their study revealed that

higher current densities led to less desirable coating appearances and weaker adhesion to the substrate. They also observed that lower current densities favored higher cobalt content over iron due to differing reaction paths. Notably, coatings from lower current densities exhibited smoother surfaces, while those from higher ones displayed increased microcracks. This phenomenon was attributed to internal stress, hydrogen evolution, and mechanical interactions between the film and the substrate. Additionally, higher current densities resulted in smaller grain sizes and impacted the microhardness of the coatings. The same pattern research by Zhang et al. [30] delved into the complex dynamics between current density and the co-deposition behavior of nickel and cobalt. Their study unveiled significant fluctuations in cobalt content across different bath configurations, demonstrating the profound role of current density. Cobalt content surged remarkably within the simple chloride bath, reaching a maximum of 0.2 mA/cm², where it peaked at 67.8%. As current density increased further, cobalt content gradually declined, ultimately aligning with the reference line representing the cobalt content in the bath at 100 mA/cm². Interestingly, shifts in current efficiency were intertwined with these cobalt content trends. Elevation in current density increased efficiency associated with nickel-cobalt co-deposition within the simple chloride bath. This efficiency reached remarkable 96-98% values within the current density range of 5 to 100 mA/cm². However, this positive trajectory was offset by a subsequent decline beyond this range as current density continued to rise. This intricate investigation underscores the vital relationship between current density and cobalt content, highlighting the imperative nature of meticulous parameter optimization for effective regulation of the compositional attributes of electrodeposited alloys.The collective findings underscore the intricate relationship between current density, deposition characteristics, microstructure, and material properties in electrodeposition processes.

5.2 Bath Temperature

Higher bath temperatures can enhance the mobility of ions, leading to an increase in deposition rates and smoother coatings. Elevated temperatures can also influence the nucleation and growth of grains, affecting the microstructure and crystalline phases formed. But most of the authors have electrodeposited at room temperature. Wu et al.[31] investigated to elucidate the impact of bath temperature on the electrodeposition of the Re-Ir-Ni alloy system. Their study encompassed temperature variations across distinct points, specifically 50°C, 60°C, and 70°C. Notably, at the lower temperatures of 50°C and 60°C, the resultant coatings exhibited a noticeable absence of Ir

content. This intriguing observation was coupled with a more negative deposition overpotential, indicating a complex interplay between kinetics and temperature. This phenomenon can be attributed to the restricted deposition of Ir^{3+} ions in alkaline aqueous solutions under these conditions. As the temperature was raised to 70°C, a striking transformation occurred. The atomic composition of Ir within the coatings demonstrated a substantial increase, stabilizing at around 13–14 at%. A similar trend was observed for Ni-content, which increased from 42 at% at lower temperatures to approximately 54 at% at higher temperatures. Conversely, Re-content showcased an opposite trend. The combined (Ir + Re)-content exhibited moderate temperature sensitivity.

Berretti et al.[32] investigated the electrodeposition of significant aluminum coatings on a brass substrate using 1-butyl-3-methylimidazolium chloride ((Bmim)Cl)/$AlCl_3$ (40/60 mol%) ionic liquid solution. By conducting electrodeposition at three distinct temperatures: 50°C, 70°C, and 90°C, the author observed the effect of thermal conditions on the reduction process. Temperature increases favored lesser surface roughness (Table 3) and more homogeneous microstructure. The SEM morphology (Figure 3) demonstrates the transition from pinnacle-type deposits at 50°C to a uniform crystalline structure at 90°C

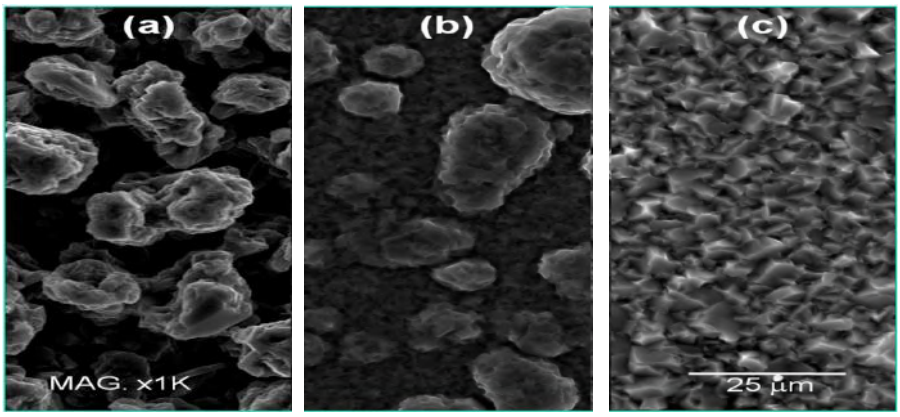

Figure 3: SEM images of Al coatings obtained at three distinct temperatures: (a) 50°C, (b) 70°C, (c) 90°[32].

Table 3. Roughness parameters for samples collected at various temperatures [32]

Sample	Rt (μm)	Ra	RzISO (μm)	Rz (μm)
Temp. 50°C	32.9 ± 1.2	3.7 ± 1.1	25.5 ± 4.1	23.3 ± 2.8
Temp. 70°C	21.7 ± 10.5	2.1 ± 0.2	14.9 ± 4.1	13.4 ± 2.8
Temp. 90°C	4.2 ± 0.1	0.3 ± 0.1	3.1 ± 0.1	2.90 ± 0.1

5.3 pH Level

pH levels can significantly impact the electrochemical reactions occurring at the electrode surface. Proper pH control can ensure stable and uniform deposition rates, preventing the formation of unwanted secondary phases. For the electrodeposition of high entropy alloy systems, researchers often used an electrolyte bath with pH values ranging from 1.5 to 2 [24]. During electrodeposition, a very pH-dependent intermediate process produces metal hydroxide ions. According to earlier research, lowering the pH during coating reduces the current efficiency and the number of components with low reduction potential [20]. Due to the high proton concentration at low pH, a significant percentage of the current is used for proton reduction, lowering the overall current efficiency. During electrodeposition, H_2 gas forms at the cathode due to an aqueous medium. Higher pH can create hydroxides, potentially causing cracks. Boric acid stabilizes pH, reducing crack formation and ensuring a uniform process. pH control and boric acid improve coating quality, adhesion, and performance [20].

In the investigation conducted by [20], the influence of varying pH levels (0.5, 1.5, 2.5, and ≥ 3.5) on the electrodeposition of FeCoNiCuZn HEA thin films was explored. Notably, lower pH values (0.5 and 1.5) were found to promote the preferential deposition of Cu. As the pH was elevated to 2.5, the quality of the deposited FeCoNiCuZn HEA films was enhanced. However, at elevated pH levels (≥ 3.5), the emergence of visible cracks raised concerns regarding the structural integrity of the electrodeposited thin films. The SEM morphology at different pH is shown in Figure 4.

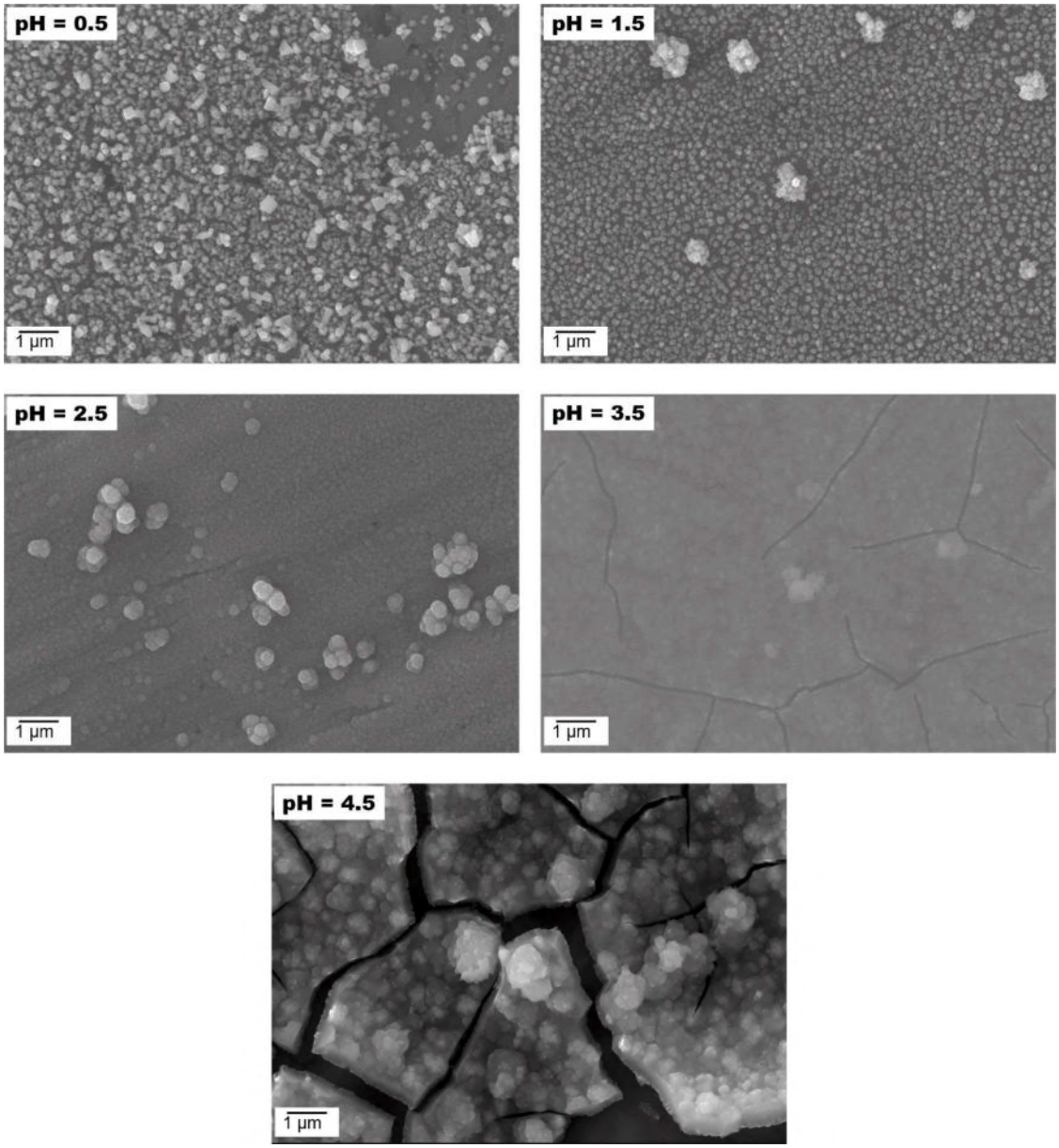

Fig 4. SEM Micrographs of electrodeposited FeCoNiCuZn at different pH conditions [20].

5.4 Agitation

Proper stirring of the electrolyte solution is crucial to ensure uniform ion dispersion on the cathode surface and facilitate mass transfer. Insufficient agitation may lead to uneven coatings and alterations in composition. Given the intricate nature of the high entropy alloy electrolyte, it is vital to thoroughly incorporate metal salts and additives. The stirring process enables complete mixing and chemical reactions, thereby increasing the metal concentration in the electrolyte. This, in turn, helps compensate for the loss of metal ions occurring at the cathode surface during

electrodeposition. Moreover, adequate stirring reduces the formation of gas bubbles, mitigating the risk of pit formation in the coating. Mamaghani et al.[33] investigated the effect of current density and stirring rate on the electroplating process in depth. The investigation was divided into two stages: first, different current densities (3, 5, 7, and 9 A/dm^2) were used, followed by the optimal current density of 5 A/dm^2 in the second stage. A magnetic stirrer was placed in the center of the bath solution and stirred at rates ranging from 100 to 500 rpm. The researchers examined how changing the current density and stirring rate affected the crystallite size, mechanical characteristics, and corrosion behavior of a nanocrystalline pure nickel covering. Notably, increasing current density and stirring rate led to smaller crystallites, with the smallest size measured at 5 A/dm2 current density and 500 rpm swirling rate (Figure 6). Furthermore, as seen in Figs. 5(a) and 5(b), stirring had a visible effect on the microstructure, resulting in cracks in the coating. Blisters were also seen within the network of cracks in Fig. 5(b). On the other hand, the specimen in Fig. 5(c) revealed a relatively homogenous structure characterized by fine crystallites when subjected to the maximum stirring rate. While stirring did not affect corrosion resistance, it did affect the corrosion current of the coating. The study proposed using the lowest ideal current density and stirring rate, particularly 5 A/dm^2 and 400 rpm, for cost-effective and well-structured production to minimize energy consumption and achieve proper crystalline structure. Stirring in the bath solution resulted in uniform microhardness distribution on the coated profile, with 400 rpm determined to be the optimum stirring rate for producing homogeneous hardness distribution.

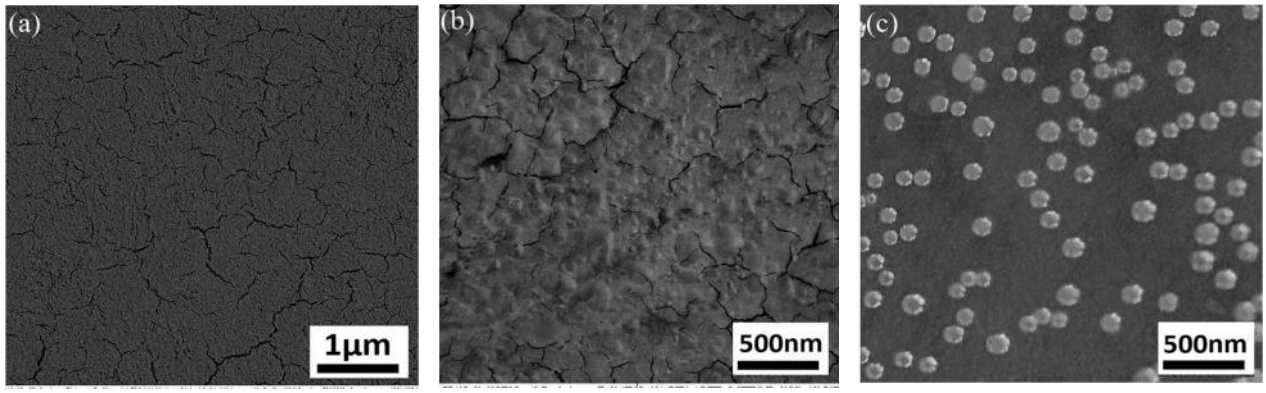

Fig 5. Morphology of nickel coatings at a current density of 5 A/dm^2. (a) No agitation, (b) 300 rpm, and (c) 500 rpm stirring rates in the solution.[33]

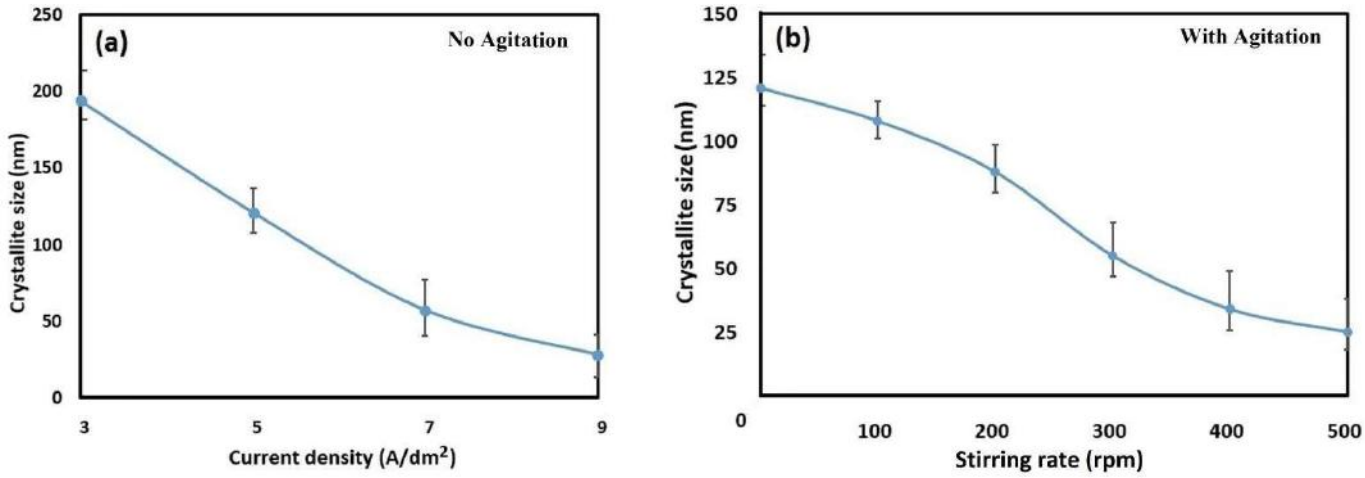

Fig 6 Crystallite size variation: (a) in the stationary bath at different current densities (stirring rate = 0 rpm), (b) at 5 A/dm^2 current density with varied stirring rates [33].

5.5 Deposition Time

In the context of electrodeposition for HEAs, the effect of deposition time on coating properties emerges as a significant variable. The studies conducted by Mulyadi et al. and Chen et al. shed light on how the duration of deposition time influences coating characteristics. While associated with thicker coatings, extended deposition times introduce potential challenges such as grain coarsening and adhesion concerns. In the research by Mulyadi et al. [34], electrodeposition of FeCoNi was carried out at different deposition times: 5, 10, 20, 35, and 50 minutes. An optimal point was found at a deposition time of 20 minutes, yielding a deposition rate of 0.00214 mg/cm^{2}s and a noteworthy current efficiency of 97.00% for FeCoNi. Interestingly, this interval also revealed patterns of enhanced crystallite growth, hinting at complex crystal kinetics. Likewise, Chen et al. [35] delved into electrodeposition dynamics, examining the interplay of deposition time, current density, and scanning velocity. The optimized trio of 20-minute deposition time, 70 A/dm^2 current density, and 10 mm/s scanning speed yielded significant results. This optimized combination yielded a material deposition rate of 1.45 mg/min, a substantial coating microhardness of 532.40 HV, and a refined surface roughness of 85 nm. Beyond material attributes, it led to improved adhesion (26.12 N) and corrosion resistance (5.718 10^{-3} Acm^2). Collectively, these studies provide insights into the intricate influence of deposition time on

tailored HEA coatings, underscoring its role in controlled material synthesis. The interplay between deposition time and coating characteristics enriches the understanding of HEA electrodeposition dynamics, contributing valuable insights for advancing coating technology with precision.

6. Conclusion

This chapter explored the multiple fields of electrodeposition of HEAs, revealing the method's potential to transform the coatings and materials engineering field. Researchers can develop coatings with tuned properties due to the convergence of electrodeposition techniques, a variety of electrolyte baths, and the adjustment of deposition settings, opening up possibilities for crucial applications in various sectors. As the field advances, the continued exploration of deposition parameters, alloy compositions, and the synergy between electrodeposition and HEAs holds immense promise for unlocking the full potential of these exceptional alloys.

References

[1] J. W. Yeh *et al.*, "Nanostructured high-entropy alloys with multiple principal elements: Novel alloy design concepts and outcomes," *Adv. Eng. Mater.*, vol. 6, no. 5, pp. 299–303, 2004, doi: 10.1002/adem.200300567.

[2] B. Cantor, I. T. H. Chang, P. Knight, and A. J. B. Vincent, "Microstructural development in equiatomic multicomponent alloys," *Mater. Sci. Eng. A*, vol. 375–377, no. 1-2 SPEC. ISS., pp. 213–218, 2004, doi: 10.1016/j.msea.2003.10.257.

[3] O. N. Senkov, G. B. Wilks, J. M. Scott, and D. B. Miracle, "Mechanical properties of Nb25Mo25Ta 25W25 and V20Nb20Mo 20Ta20W20 refractory high entropy alloys," *Intermetallics*, vol. 19, no. 5, pp. 698–706, 2011, doi: 10.1016/j.intermet.2011.01.004.

[4] M. H. Tsai and J. W. Yeh, "High-entropy alloys: A critical review," *Mater. Res. Lett.*, vol. 2, no. 3, pp. 107–123, 2014, doi: 10.1080/21663831.2014.912690.

[5] Y. Zhang *et al.*, "Microstructures and properties of high-entropy alloys," *Prog. Mater. Sci.*, vol. 61, no. September 2013, pp. 1–93, 2014, doi: 10.1016/j.pmatsci.2013.10.001.

[6] D. B. Miracle and O. N. Senkov, "A critical review of high entropy alloys and related concepts," *Acta Mater.*, vol. 122, pp. 448–511, 2017, doi: 10.1016/j.actamat.2016.08.081.

[7] Z. Rong *et al.*, "Microstructure and properties of FeCoNiCrX (X[dbnd]Mn, Al) high-entropy alloy coatings," *J. Alloys Compd.*, vol. 921, p. 166061, 2022, doi: 10.1016/j.jallcom.2022.166061.

[8] A. Sharma, "High entropy alloy coatings and technology," *Coatings*, vol. 11, no. 4, 2021, doi: 10.3390/coatings11040372.

[9] X. Zhang, C. Li, S. Zheng, Y. Di, and Z. Sun, "Ac ce p an us cri pt No op ye dit Abstract :

Ac ce p us pt No t C ye ed," vol. 62339920, 2021.

[10] A. M. J. Popescu *et al.*, "Electrodeposition, characterization, and corrosion behavior of CoCrFeMnNi high-entropy alloy thin films," *Coatings*, vol. 11, no. 11, 2021, doi: 10.3390/coatings11111367.

[11] S. B. H. Gmbh, *済無No Title No Title No Title*. 2016.

[12] B. M. Mundotiya and W. Ullah, "Electrodeposition Approaches to Deposit the Single-Phase Solid Solution of Ag-Ni Alloy", Novel Metal Electrodeposition and the Recent Application, IntechOpen, 2018. DOI: 10.5772/intechopen.80846

[13] J. A. O. Sci, "Characterizing ceramics and the interfacial adhesion to resin : ii- the relationship of surface treatment , bond strength , interfacial toughness and fractography," vol. 13, no. 2, pp. 101–109, 2005.

[14] T. Nanostructures and T. Films, "Two-Dimensional Nanostructures: Thin Films 5.1.".

[15] A. Aliyu and C. Srivastava, "Microstructure and corrosion properties of MnCrFeCoNi high entropy alloy-graphene oxide composite coatings," *Materialia*, vol. 5, no. February, 2019, doi: 10.1016/j.mtla.2019.100249.

[16] V. Soare *et al.*, "Electrochemical deposition and microstructural characterization of AlCrFeMnNi and AlCrCuFeMnNi high entropy alloy thin films," *Appl. Surf. Sci.*, vol. 358, no. July, pp. 533–539, 2015, doi: 10.1016/j.apsusc.2015.07.142.

[17] Y. F. Kao, T. D. Lee, S. K. Chen, and Y. S. Chang, "Electrochemical passive properties of AlxCoCrFeNi (x = 0, 0.25, 0.50, 1.00) alloys in sulfuric acids," *Corros. Sci.*, vol. 52, no. 3, pp. 1026–1034, 2010, doi: 10.1016/j.corsci.2009.11.028.

[18] A. Aliyu, K. Sai Jyotheender, and C. Srivastava, "Texture and grain boundary engineering in nickel coating with tungsten addition and its effect on the coating corrosion behavior," *Surf. Coatings Technol.*, vol. 412, no. March, p. 127079, 2021, doi: 10.1016/j.surfcoat.2021.127079.

[19] A. Aliyu and C. Srivastava, "Correlation between growth texture, crystallite size, lattice strain and corrosion behavior of copper-carbon nanotube composite coatings," *Surf. Coatings Technol.*, vol. 405, no. November 2020, p. 126596, 2021, doi: 10.1016/j.surfcoat.2020.126596.

[20] K. Siri, K. Janardhana, L. P. P. Chokkakula, and S. R. Dey, "Electrochimica Acta Strategies to engineer FeCoNiCuZn high entropy alloy composition through aqueous electrochemical deposition," *Electrochim. Acta*, vol. 453, no. January, p. 142350, 2023, doi: 10.1016/j.electacta.2023.142350.

[21] C. Z. Yao *et al.*, "Electrochemical preparation and magnetic study of Bi-Fe-Co-Ni-Mn high entropy alloy," *Electrochim. Acta*, vol. 53, no. 28, pp. 8359–8365, 2008, doi: 10.1016/j.electacta.2008.06.036.

[22] A. Aliyu, M. Y. Rekha, and C. Srivastava, "Microstructure-electrochemical property correlation in electrodeposited CuFeNiCoCr high-entropy alloy-graphene oxide composite coatings," *Philos. Mag.*, vol. 99, no. 6, pp. 718–735, 2019, doi:

10.1080/14786435.2018.1554915.

[23] A. Aliyu and C. Srivastava, “Microstructure-corrosion property coated AlCrFeCoNiCu high entropy alloys-graphene oxide composite coatings,” *Thin Solid Films*, vol. 686, no. December 2018, p. 137434, 2019, doi: 10.1016/j.tsf.2019.137434.

[24] A. Aliyu and C. Srivastava, “Microstructure and corrosion performance of AlFeCoNiCu high entropy alloy coatings by addition of graphene oxide,” *Materialia*, vol. 8, no. August, 2019, doi: 10.1016/j.mtla.2019.100459.

[25] A. Aliyu and C. Srivastava, “Corrosion behavior and protective film constitution of AlNiCoFeCu and AlCrNiCoFeCu high entropy alloy coatings,” *Surfaces and Interfaces*, vol. 27, no. June, p. 101481, 2021, doi: 10.1016/j.surfin.2021.101481.

[26] V. Soare *et al.*, “Electrochemical deposition and microstructural characterization of AlCrFeMnNi and AlCrCuFeMnNi high entropy alloy thin films,” *Appl. Surf. Sci.*, vol. 358, pp. 533–539, 2015, doi: 10.1016/j.apsusc.2015.07.142.

[27] Z. Zhu, H. Meng, and P. Ren, “CoNiWReP high entropy alloy coatings prepared by pulse current electrodeposition from aqueous solution,” *Colloids Surfaces A Physicochem. Eng. Asp.*, vol. 648, no. May, p. 129404, 2022, doi: 10.1016/j.colsurfa.2022.129404.

[28] A. M. J. Popescu *et al.*, “Influence of Heat Treatment on the Corrosion Behavior of Electrodeposited CoCrFeMnNi High-Entropy Alloy Thin Films,” *Coatings*, vol. 12, no. 8, 2022, doi: 10.3390/coatings12081108.

[29] Z. Ghaferi, S. Sharafi, and M. E. Bahrololoom, “Effect of current density and bath composition on crystalline structure and magnetic properties of electrodeposited FeCoW alloy,” *Appl. Surf. Sci.*, vol. 355, pp. 766–773, 2015, doi: 10.1016/j.apsusc.2015.07.083.

[30] C. Fan and D. L. Piron, “Study of anomalous nickel-cobalt electrodeposition with different electrolytes and current densities,” *Electrochim. Acta*, vol. 41, no. 10, pp. 1713–1719, 1996, doi: 10.1016/0013-4686(95)00488-2.

[31] W. Wu, N. Eliaz, and E. Gileadi, “The Effects of pH and Temperature on Electrodeposition of Re-Ir-Ni Coatings from Aqueous Solutions,” *J. Electrochem. Soc.*, vol. 162, no. 1, pp. D20–D26, 2015, doi: 10.1149/2.0281501jes.

[32] E. Berretti *et al.*, “Aluminium electrodeposition from ionic liquid: Effect of deposition temperature and sonication,” *Materials (Basel).*, vol. 9, no. 9, pp. 1–14, 2016, doi: 10.3390/ma9090719.

[33] K. R. Mamaghani and S. M. Naghib, “The effect of stirring rate on electrodeposition of nanocrystalline nickel coatings and their corrosion behaviors and mechanical characteristics,” *Int. J. Electrochem. Sci.*, vol. 12, no. 6, pp. 5023–5035, 2017, doi: 10.20964/2017.06.68.

[34] M. Mulyadi and Afrizal, “The Effects of Deposition Time on Phase and Structure of FeCoNi Films,” *Chem. Mater.*, vol. 1, no. 2, pp. 40–44, 2022, doi: 10.56425/cma.v1i2.23.

[35] Y. Chen *et al.*, “Effects of deposition current density, time and scanning velocity on scanning jet electrodeposition of Ni-Co alloy coating,” *J. Manuf. Process.*, vol. 101, no.

June, pp. 458–468, 2023, doi: 10.1016/j.jmapro.2023.06.020.